Multivalued Inverse Design: Multiple Surface Geometries from One Flat Sheet

Itay Griniasty,[1,*] Cyrus Mostajeran,[2] and Itai Cohen[1]
[1]Laboratory of Atomic and Solid State Physics, Cornell University, Ithaca, New York 14853-2501, USA
[2]Department of Engineering, University of Cambridge, Cambridge, England CB2 1PZ, United Kingdom

(Received 9 February 2021; revised 19 May 2021; accepted 4 August 2021; published 13 September 2021)

Designing flat sheets that can be made to deform into three-dimensional shapes is an area of intense research with applications in micromachines, soft robotics, and medical implants. Thus far, such sheets were designed to adopt a single target shape. Here, we show that through anisotropic deformation applied inhomogeneously throughout a sheet, it is possible to design a single sheet that can deform into multiple surface geometries upon different actuations. The key to our approach is development of an analytical method for solving this multivalued inverse problem. Such sheets open the door to fabricating machines that can perform complex tasks through cyclic transitions between multiple shapes. As a proof of concept, we design a simple swimmer capable of moving through a fluid at low Reynolds numbers.

DOI: 10.1103/PhysRevLett.127.128001

Designing shape shifting sheets is of enormous interest in fields including micromachines [1], soft robotics [2,3], and medical implants [4] where fabrication and production constraints often require an initial flat configuration. Programming a single shape transformation in such sheets already enables designs for switches, deployable structures [5], and actuators [6]. Designing sheets that can adopt multiple target geometries would open the door to more sophisticated machines that can cycle through multiple states, perform work on their surroundings, and locomote through viscous fluids [7,8].

In origami, it is possible to program more than one shape into a single sheet [9–11]. However, the shapes are almost always incompatible, which means that the sheet must return to the flat configuration before it is folded into another shape. Elastic sheets can fold from one shape to another directly [12]. Here, we show how to inverse design a sheet so that it can transform into a series of shapes in an arbitrary sequence in response to actuation signals. By transforming from one shape to another directly, without returning to its original flat configuration, such sheets are able to perform complex tasks and do work on their environment. The challenge in designing such pluripotent sheets, however, is that one must simultaneously control multiple independent degrees of freedom, such as the deformation magnitude and orientation, to obtain multiple independent shapes (Fig. 1).

Most shape shifting sheets have been designed to deform into a single target geometry via one of two deformation modalities where only one deformation degree of freedom is varied [13]: (i) inhomogeneous isotropic deformations [14,15], where the deformation magnitude varies throughout the sheet [16–19]; and (ii) homogeneous anisotropic deformations [20], where the deformation principal axis varies throughout the sheet [2,21–34]. Both modalities can be used to alter a sheet's local Gaussian curvature and determine its geometry. Importantly, the technology to simultaneously implement both modalities to achieve multiple shapes already exists [17,35]. Missing, however, is a mathematical framework to generate designs that implement both degrees of freedom to obtain the desired surfaces.

Naive combinations of the inverse design methods of homogeneous and anisotropic systems [14,15,20] generally fail at this task. The naive approach fails because the local Gaussian curvature of an actuated sheet is nonlinearly dependent on both degrees of freedom. The curvature is, however, linear in the highest order derivatives of the deformation degrees of freedom. Therefore, it may be possible to rephrase the inverse design problem as a system of partial differential equations (PDEs) in the deformation degrees of freedom, where the actuated sheet's curvatures equal those of the target surfaces, and use linearity to simultaneously solve the equations.

Implementing this strategy requires formulating a common description of the initial and target surfaces in terms of a shared coordinate system. A sheet's deformation is characterized by its principal axis with respect to the initial sheet, denoted by a director $\hat{\mathbf{n}}$, and the deformation magnitudes along and across the director of λ_1 and λ_2, respectively. Generally, λ_1, λ_2, and $\hat{\mathbf{n}}$ can all depend on external time dependent actuation stimuli $\mathbf{\Lambda}(t)$ that drive the deformation. Most known anisotropically deforming systems, however, are *uniaxial*: their deformation's principal axis $\hat{\mathbf{n}}$ is independent of the actuation $\mathbf{\Lambda}$ [2,21–34,36]. In such materials, the integral curves of the principal axis $\hat{\mathbf{n}}$ and its perpendicular $\hat{\mathbf{n}}_\perp$ form a "material" coordinate system (u, v) on the sheet throughout the deformation such that

$$\partial_u \mathbf{r}_{\mathbf{\Lambda}} = \alpha\lambda_1 \hat{\mathbf{n}}_{\mathbf{\Lambda}}, \qquad \partial_v \mathbf{r}_{\mathbf{\Lambda}} = \beta\lambda_2 \hat{\mathbf{n}}_{\mathbf{\Lambda}\perp}, \tag{1}$$

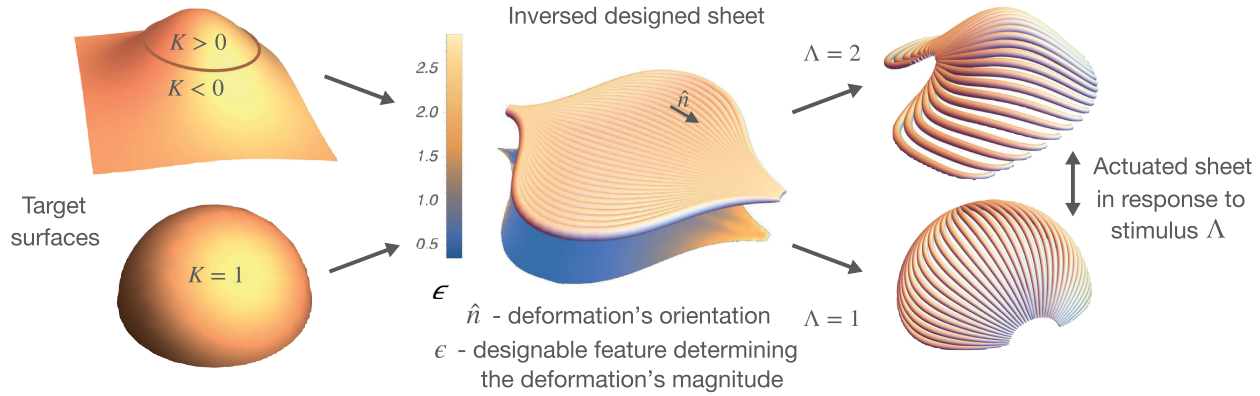

FIG. 1. Inverse design of pluripotent sheets. Left, target surfaces with defined Gaussian curvatures K. Center, inverse designed sheet, where $\hat{\mathbf{n}}$ specifies deformation's orientation and ϵ is an experimentally accessible system feature controlling the deformation's magnitude, which is designed with $\hat{\mathbf{n}}$ such that the sheet deforms into the target surfaces. Right, actuated sheet deforming into multiple target surfaces in response to different values of the stimulus Λ.

where $\mathbf{r}_\Lambda$ are the coordinates of the sheet for an actuation $\mathbf{\Lambda}$, α and β are the arc lengths of u and v parametric curves on the initial sheet, and $\hat{\mathbf{n}}_\Lambda$ are the images of the director $\hat{\mathbf{n}}$ on the deformed surfaces (Fig. 2). The deformation magnitudes are also functions of designable features $\boldsymbol{\epsilon}(u, v)$ specified on the undeformed sheet. Thus, the sheet's geometries throughout the deformation are given by the metrics

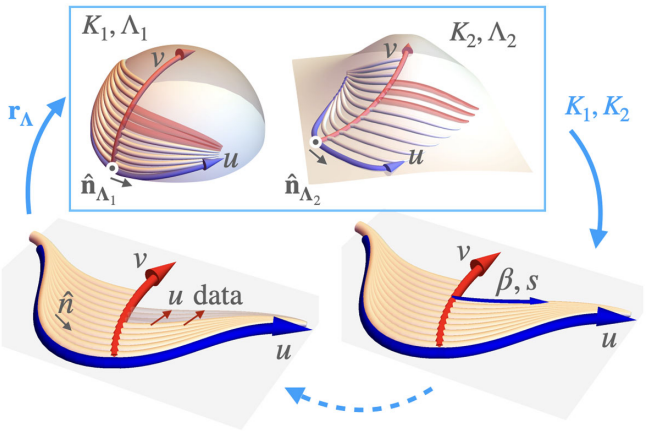

FIG. 2. Inverse design scheme of a flat uniaxial sheet with a designable elastic response $[\lambda_1(\epsilon) \neq \text{const}]$ for two target surfaces with Gaussian curvatures K_1 and K_2 in response to stimuli Λ_1 and Λ_2. (u, v) coordinates given by integral curves of deformation's anisotropy axis $\hat{\mathbf{n}}$ or $\hat{\mathbf{n}}_\perp$ are shared by all surfaces and allow derivation of a system of equations describing the inverse problem. Numerical integration of this inverse problem is given by iteration of the following integration steps: Bottom left, given complete data on a director integral curve, u data $= (\mathbf{r}_\Lambda, \hat{\mathbf{n}}_\Lambda, \alpha, b, \epsilon, q)$ is propagated a step dv along the director perpendicular, forming a new director integral curve. Top, curvature of target surfaces along new director integral curve is obtained. Bottom right, initial data for β and s, given on initial director-perpendicular curve, are integrated along new director integral curve to complete the data on it.

$$ds^2(\mathbf{\Lambda}) = \lambda_1^2(\mathbf{\Lambda}, \boldsymbol{\epsilon})\alpha^2 du^2 + \lambda_2^2(\mathbf{\Lambda}, \boldsymbol{\epsilon})\beta^2 dv^2. \tag{2}$$

This shared coordinate system can then be used to define the Gaussian curvatures of multiple actuated surfaces simultaneously.

An actuated sheet's Gaussian curvature is a function of the deformation degrees of freedom expressed in the metric [Eq. (2)] and its derivatives. For a surface with orthogonal coordinates defined by Eq. (1), the Gaussian curvature is given by [37]

$$K = \hat{\mathbf{n}}_\perp \cdot \nabla \kappa_{gu} - \hat{\mathbf{n}} \cdot \nabla \kappa_{gv} - \kappa_{gu}^2 - \kappa_{gv}^2.$$

where κ_{gu} and κ_{gv} are geodesic curvatures of u and v parametric curves, which are themselves PDEs in the designable director:

$$\kappa_{gu}\hat{\mathbf{n}}_\perp = \hat{\mathbf{n}} \cdot \nabla \hat{\mathbf{n}}, \qquad \kappa_{gv}\hat{\mathbf{n}}_\perp = \hat{\mathbf{n}}_\perp \cdot \nabla \hat{\mathbf{n}}, \tag{3}$$

Keeping in mind that we would eventually like to design the sheet properties, we express the geodesic curvatures, κ_{gu} and κ_{gv}, as functions of the designable elastic features $\boldsymbol{\epsilon}$, as well as α and β, which uniquely determine the designable director $\hat{\mathbf{n}}$ [37] [see Supplemental Material (SM) for derivation [38]]:

$$\kappa_{gu} = \frac{b}{\lambda_2} - \frac{\partial \lambda_1}{\lambda_1 \partial \boldsymbol{\epsilon}} \frac{\mathbf{q}}{\lambda_2}, \qquad \kappa_{gv} = \frac{s}{\lambda_1} + \frac{\partial \lambda_2}{\lambda_2 \partial \boldsymbol{\epsilon}} \frac{\mathbf{p}}{\lambda_1},$$
$$b = -\frac{\partial_v \alpha}{\alpha\beta}, \quad s = \frac{\partial_u \beta}{\alpha\beta}, \quad \mathbf{p} = \frac{\partial_u \boldsymbol{\epsilon}}{\alpha} \quad \text{and} \quad \mathbf{q} = \frac{\partial_v \boldsymbol{\epsilon}}{\beta}. \tag{4}$$

Derivatives along and across the director are expressed with respect to u and v: $\hat{\mathbf{n}} \cdot \nabla = (1/\lambda_1\alpha)\partial_u$ and $\hat{\mathbf{n}}_\perp \cdot \nabla = (1/\lambda_2\beta)\partial_v$. Using Eq. (4), we can thus express the Gaussian curvature as a quasilinear first order equation in b, s, $\mathbf{p}$, and $\mathbf{q}$:

$$K = \frac{1}{\lambda_2\beta}\frac{\partial}{\partial v}\left(\frac{b}{\lambda_2} - \frac{\partial\lambda_1}{\lambda_1\partial\boldsymbol{\epsilon}}\frac{\mathbf{q}}{\lambda_2}\right) - \frac{1}{\lambda_1\alpha}\frac{\partial}{\partial u}\left(\frac{s}{\lambda_1} + \frac{\partial\lambda_2}{\lambda_2\partial\boldsymbol{\epsilon}}\frac{\mathbf{p}}{\lambda_1}\right) - \left(\frac{s}{\lambda_1} + \frac{\partial\lambda_2}{\lambda_2\partial\boldsymbol{\epsilon}}\frac{\mathbf{p}}{\lambda_1}\right)^2 - \left(\frac{b}{\lambda_2} - \frac{\partial\lambda_1}{\lambda_1\partial\boldsymbol{\epsilon}}\frac{\mathbf{q}}{\lambda_2}\right)^2. \quad (5)$$

The quantities b, s, $\mathbf{p}$, and $\mathbf{q}$ (and, by extension, the Gaussian curvature) are thus determined by $\boldsymbol{\epsilon}$, α, and β.

Since $\boldsymbol{\epsilon}$, α, and β are independent, the relations in Eq. (4) allow for the simultaneous satisfaction of Eq. (5) for multiple surface geometries. To obtain solutions, this system of PDEs must be diagonalized and shown to be integrable. We illustrate this procedure for a flat sheet that deforms into two different target shapes, and we show how it naturally extends for an arbitrary number of target shapes.

Inverse design of two target surfaces.—Consider a uniaxial sheet with a single scalar designable feature ϵ affecting the deformation such that, without loss of generality [39], $\partial_\epsilon\lambda_1 \neq 0$. The curvatures of the initial sheet and two target surface geometries $\mathbf{K} = [K_0(\mathbf{r}_{\Lambda_0}), K_1(\mathbf{r}_{\Lambda_1}), K_2(\mathbf{r}_{\Lambda_2})]$ define three PDEs in ϵ, α, and β. The equations are linear in $\partial_v b$, $\partial_u s$, $\partial_u p$, and $\partial_v q$. The variations of ϵ, $\partial_u p$, and $\partial_v q$, however, are not independent; and, as shown in the SM [38], $\partial_v q$ determines $\partial_u p$ given a Cauchy problem [40]. Recasting Eq. (5) in terms of the unknown highest order terms

$$\begin{aligned} \bar{\mathbf{K}} &= \mathbf{K} - \mathbf{M}\cdot\mathbf{d}, \\ M_i(\Lambda_i) &= \left(\tfrac{1}{\lambda_2^2}, \quad -\tfrac{1}{\lambda_1^2}, \quad -\tfrac{\partial\log\lambda_1}{\lambda_2^2\partial\epsilon}\right), \quad i \in \{1,2,3\}, \\ \mathbf{d} &= \left(\tfrac{1}{\beta}\partial_v b, \quad \tfrac{1}{\alpha}\partial_u s, \quad \tfrac{1}{\beta}\partial_v q\right), \end{aligned} \quad (6)$$

it is possible to determine $\partial_v b$, $\partial_u s$, and $\partial_v q$ in terms of $\bar{\mathbf{K}}$, which are functions of α, β, ϵ, p, q, b, s, $\partial_u p$ and the prescribed target curvatures $\mathbf{K}$:

$$\mathbf{d} = \mathbf{M}^{-1}\cdot(\mathbf{K} - \bar{\mathbf{K}}). \quad (7)$$

Equations (1), (3), (4), and (7) form a system of PDEs whose solution is a uniaxial sheet that deforms into the two desired target surfaces, realizing their prescribed metrics, upon actuations Λ_1 and Λ_2 (see Fig. 1). Supplemented by analytical initial conditions, this system is complete and integrable [38,41,42]. Furthermore, if one of the deformation magnitudes is insensitive to ϵ, which is the case for existing implementations of uniaxial sheets [17,35], the system of equations is hyperbolic; and a solution can be integrated from initial conditions for a substantial domain [43].

It is illuminating to find solutions of the inverse problem, $\boldsymbol{\epsilon}(\mathbf{r})$ and $\hat{\mathbf{n}}(\mathbf{r})$, by integrating a Goursat-like problem [44] as depicted in Fig. 2. Initial data consist of a position and director on each target surface, which are accompanied by u and v curves on the initial surface, where data propagating across each curve are given on it. That is, data for (α, b, ϵ, q) are given on the u curve, and data for (β, s) are given on the v curve. A solution is then found by iteratively propagating the data along u and v. The variables $u\,\text{data} \equiv (\alpha, \epsilon, b, p, \partial_v p, q, \{\mathbf{r}_{\mathbf{\Lambda}_i}, \hat{\mathbf{n}}_{\mathbf{\Lambda}_i}\}_{i=0}^2)$ are propagated a step dv, forming a new u curve. Next, the curvatures of the target surfaces $[K_1(\mathbf{r}_{\Lambda_1}), K_2(\mathbf{r}_{\Lambda_2})]$ are obtained along the new curve. With these curvatures, we obtain the values of $\partial_u s$ through Eq. (7), which we integrate to obtain s and β along the new u curve, completing the data on it. The integration steps are iterated until a global solution $\epsilon(\mathbf{r}), \hat{\mathbf{n}}(\mathbf{r})$ of the inverse problem is found, or until a singularity forms: $\alpha = 0$; $\beta = 0$; or for all applied stimuli, $\lambda_1 = \lambda_2$.

Singularities.—The first two singularities where α or β vanish are defects in the nematic texture discussed in [20]. The third ($\lambda_1 = \lambda_2$ for all applied stimuli) is an isotropic point. At such a point, variations of the director no longer affect the deformation; and the sheet cannot be designed to obtain all target curvatures simultaneously. The appearance of singularities may be delayed by varying the initial conditions such that greater coverage of the target surfaces is achieved [20].

Inverse design of multiple surfaces.—In general, if there are N designable features $\boldsymbol{\epsilon}$ independently affecting a uniaxial sheet's deformation, then the sheet may be designed to morph into $N+1$ independent surfaces. Here, the inverse design procedure is nearly identical to that of a sheet morphing into two shapes. The key difference is that because there are multiple designable features, we can no longer assume that they all affect the deformations along the director. For example, if ϵ_1 affects only the deformation along the director λ_1 while ϵ_2 affects only the deformation across it λ_2, then the variations of ϵ_1 across the director and ϵ_2 along it ($\partial_v q_1$ and $\partial_u p_2$) are relevant to their inverse design; whereas $\partial_u p_1$ and $\partial_v q_2$ are not. Equation (6) then needs to be modified to account for the relevant highest order terms $\mathbf{d}$, which now include $\partial_v b$, $\partial_u s$, and a mix of $\partial_u p_i$ and $\partial_v q_j$. The coefficients matrix $\mathbf{M}$ is then appropriately redefined such that, after subtracting $\mathbf{M}\cdot\mathbf{d}$ from the curvature $\mathbf{K}$, the remainder $\bar{\mathbf{K}}$ is no longer a function of the relevant highest order derivatives. The accordingly modified Eq. (7) together with Eqs. (1), (3), and (4) then composes a complete, integrable system of equations whose solutions are sheets deforming into $N+1$ target surfaces. The detailed derivation of the equations and an integration scheme are given in the SM [38].

Multiple independent stimuli.—The formulation of the inverse problem and the above integration scheme also hold when the deformation occurs in response to multiple independent stimuli, such as light, pressure, or heat: $\mathbf{\Lambda} = (\Lambda^1, \ldots, \Lambda^k)$. An example of a solution to such a multitarget inverse problem is presented in Fig. 3. The sheet depicted has two designable features separately affecting its deformation magnitudes in response to independent

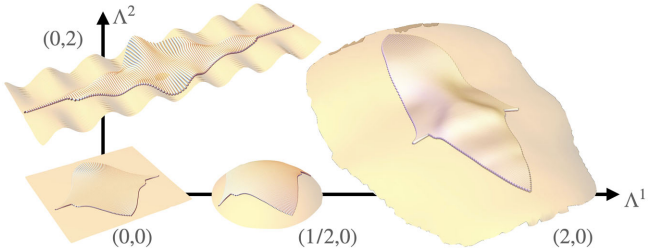

FIG. 3. Inverse design of multiple shapes. A flat uniaxial sheet with two designable system features [$\lambda_i = \exp(\epsilon_i \Lambda^i), i \in \{1,2\}$] is designed to deform into three target shapes in response to two stimuli Λ^1 and Λ^2. The sheet deforms into a sphere and then a facelike mask in response to Λ^1 and into a wavy sheet in response to Λ^2. Maximal strains are below 300% and are within experimental reach [45].

stimuli: $\lambda_1(\Lambda^1, \epsilon_1)$ and $\lambda_2(\Lambda^2, \epsilon_2)$. Such a sheet can morph into highly distinct surfaces. In response to Λ^1, the sheet extends along $\hat{\mathbf{n}}$ and morphs first into a sphere of constant curvature, and then into a face with a complex curvature profile. In response to Λ^2, the sheet morphs across $\hat{\mathbf{n}}$ into a surface oscillating along two orthogonal coordinates with two different periods. The sheet can then transform into the face, without going through the sphere, by simultaneously changing both stimuli and extending along $\hat{\mathbf{n}}$ while contracting across it. This example illustrates a general feature: the *path* in shape space of a sheet morphing between target geometries in response to multiple independent stimuli can be manipulated in a nontrivial manner.

Locomotion and work.—Cycling between multiple shapes is a standard method of doing work and performing complex tasks. It is of particular importance in microscopic machines (such as swimmers) that, due to their size, operate in settings where viscous forces dominate inertial forces, resulting in instantaneous flows that have "no memory." As a consequence, only nonreciprocal motions give rise to a net propulsion [46]. We provide a simple design for a composite sheet that is capable of locomotion in such environments (Fig. 4). The composite sheet consists of two homogeneous layers with independently controllable, orthogonal, director patterns whose actuated Gaussian curvatures are opposite [Fig. 4(a)]. When the sheets are sequentially actuated and then simultaneously relaxed, they execute a simple nonreciprocal work cycle [Fig. 4(b)] [25] that results in an overall translation along the axis of symmetry [Fig. 4(c)].

This locomotion is powered by the work that the sheet does on its environment. For any actuation, this work is bounded by the frustrated elastic energy [48] that would build up if the sheet was constrained to stay in its initial configuration. Because we have defined a common coordinate system, we can integrate the energy density along the target surfaces to obtain this bound,

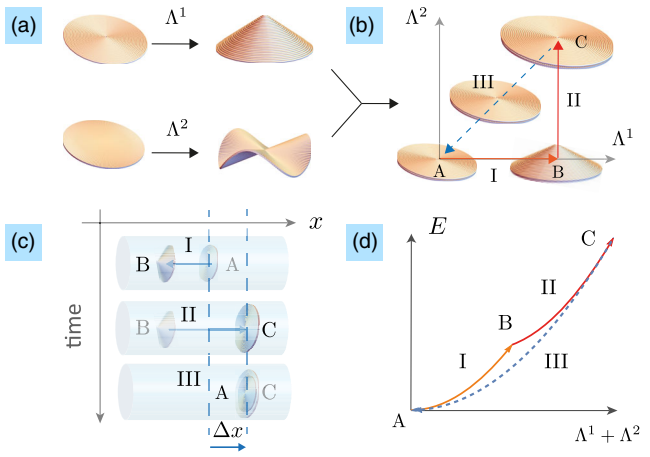

FIG. 4. (a) Bilayered uniaxial sheet composed of a top layer with an azimuthal director pattern and a bottom layer with the orthogonal radial director pattern. Top and bottom layers deform into cones and anticones upon actuation, respectively [47]. (b) Nonreciprocal cycle of shape transformations between multiple flat and conical shapes in the bilayered design through the use of two independently controllable stimuli Λ^1 and Λ^2 and the corresponding cycle in parameter space. (c) Locomotion of a swimmer at low Reynolds number with net displacement Δx achieved during each cycle. (d) Bounds on work [E from Eq. (8)] that system can perform on its surroundings at each stage of cycle.

$$E = h \iint_{\text{Target Surface}} \mathcal{E}(\lambda_1, \lambda_2) dA, \tag{8}$$

where h is the sheet's (unactivated) thickness, and the energy density $\mathcal{E}$ on a target surface is derived in the SM [38]. Finally, although we have used all the deformation degrees of freedom to obtain the target surfaces, we can still vary the initial conditions to control the sheet's capacity to do work along a prescribed curve on the target surface. Such control may find applications in the design of lifters [6]: for instance, where a greater concentration of elastic energy at points of contact may be advantageous. Collectively, the ability to use this inverse design approach to design a sheet that can morph into multiple surfaces capable of executing locomotion and even concentrating elastic energy at specific locations is quite remarkable.

Discussion.—By systematically utilizing multiple degrees of freedom to program a single sheet of material so that it can transform into multiple target geometries, we have provided a vital theoretical foundation for the design of printable sheets capable of executing complex behaviors. The inverse design of a specific system using this approach is straightforward. One needs to (i) specify the set of designable features and how they affect the deformation magnitudes in response to stimuli, (ii) select a compatible number of target surfaces to be obtained at specified actuation values, and (iii) choose initial conditions for the integration procedure.

Using these inputs, the code [49] produces designs for the director $\hat{\mathbf{n}}$ and designable features ϵ.

Candidate systems for the implementation of this design modality include (i) liquid crystal elastomers, where the deformation's orientation and magnitude can be controlled by varying the nematic director's in-plane and out-of-plane orientation [27,50], or the extent of deformation in response to the nematic phase transition [51]; (ii) four-dimensionally printed hydrogels, anisotropically deforming along aligned cellulose fibrils, whose orientation in and out of the plane similarly control the deformation's orientation and magnitude; and (iii) microrobotic kirigami metamaterial sheets where the deformation's orientation and magnitude can be controlled by varying the local bending of chemical or electrochemical actuators [1,52–54]. In each of these examples, the deformations are typically applied globally. As fabrication techniques improve, it may be possible to control the actuation at each point along the surface independently. In this scenario, we can use the inverse design framework developed here to obtain the desired target shape by treating the actuation as a designable feature. Such designable local actuations would allow a single sheet to update its target curvatures on the fly and morph into almost any desired surface geometry in real time.

We thank James Sethna for insightful discussions. This work was supported by the U.S. Army Research Office (W911NF-18-1-0032), the National Science Foundation (EFMA-1935252), and the Cornell Center for Materials Research (DMR-1719875). I. G. also received partial support from the Cornell Laboratory of Atomic and Solid State Physics. C. M. was supported by Fitzwilliam College and a Henslow Research Fellowship from the Cambridge Philosophical Society.

*itaygrin@gmail.com

[1] M. Z. Miskin, A. J. Cortese, K. Dorsey, E. P. Esposito, M. F. Reynolds, Q. Liu, M. Cao, D. A. Muller, P. L. McEuen, and I. Cohen, Nature (London) **584**, 557 (2020).
[2] E. Reyssat and L. Mahadevan, J. R. Soc., Interface **6**, 951 (2009).
[3] T. J. Wallin, J. Pikul, and R. F. Shepherd, Nat. Rev. Mater. **3**, 84 (2018).
[4] A. J. T. Teo, A. Mishra, I. Park, Y.-J. Kim, W.-T. Park, and Y.-J. Yoon, ACS Biomater. Sci. Eng. **2**, 454 (2016).
[5] D. J. Hartl and D. C. Lagoudas, Proceedings of the Institution of Mechanical Engineers, Part G (Journal of Aerospace Engineering) **221**, 535 (2007).
[6] T. Guin, M. J. Settle, B. A. Kowalski, A. D. Auguste, R. V. Beblo, G. W. Reich, and T. J. White, Nat. Commun. **9**, 2531 (2018).
[7] S. Palagi and P. Fischer, Nat. Rev. Mater. **3**, 113 (2018).
[8] I. Levin, R. Deegan, and E. Sharon, Phys. Rev. Lett. **125**, 178001 (2020).
[9] E. D. Demaine and T. Tachi, in *Proceedings of the 33rd International Symposium on Computational Geometry (SoCG 2017), Brisbane, Australia* (Schloss Dagstuhl-Leibniz-Zentrum fuer Informatik, 2017).
[10] J.-H. Na, A. A. Evans, J. Bae, M. C. Chiappelli, C. D. Santangelo, R. J. Lang, T. C. Hull, and R. C. Hayward, Adv. Mater. **27**, 79 (2015).
[11] Q. Liu, W. Wang, M. F. Reynolds, M. C. Cao, M. Z. Miskin, T. A. Arias, D. A. Muller, P. L. McEuen, and I. Cohen, Sci. Rob. **6**, eabe6663 (2021).
[12] R. K. Manna, O. E. Shklyaev, H. A. Stone, and A. C. Balazs, Mater. Horiz. **7**, 2314 (2020).
[13] C. Modes and M. Warner, Phys. Today **69**, No. 1, 32 (2016).
[14] A. Korn, *Mathematische Abhandlungen Hermann Amandus Schwarz*, edited by C. Carathéodory, G. Hessenberg, E. Landau, and L. Lichtenstein (Springer, Berlin, 1914), p. 215.
[15] L. Lichtenstein, Bull. Acad. Sci. Cracovie, Cl. Sci. Math. Nat. Ser. A 192 (1916).
[16] J. Kim, J. A. Hanna, M. Byun, C. D. Santangelo, and R. C. Hayward, Science **335**, 1201 (2012).
[17] J. H. Pikul, S. Li, H. Bai, R. T. Hanlon, I. Cohen, and R. F. Shepherd, Science **358**, 210 (2017).
[18] J. Kim, J. A. Hanna, R. C. Hayward, and C. D. Santangelo, Soft Matter **8**, 2375 (2012).
[19] Y. Klein, E. Efrati, and E. Sharon, Science **315**, 1116 (2007).
[20] I. Griniasty, H. Aharoni, and E. Efrati, Phys. Rev. Lett. **123**, 127801 (2019).
[21] A. Fahn and M. Zohary, Phytomorphology **5**, 99 (1955).
[22] S. Armon, E. Efrati, R. Kupferman, and E. Sharon, Science **333**, 1726 (2011).
[23] H. Aharoni, Y. Abraham, R. Elbaum, E. Sharon, and R. Kupferman, Phys. Rev. Lett. **108**, 238106 (2012).
[24] H. Aharoni, E. Sharon, and R. Kupferman, Phys. Rev. Lett. **113**, 257801 (2014).
[25] C. Mostajeran, Phys. Rev. E **91**, 062405 (2015).
[26] A. Sydney Gladman, E. A. Matsumoto, R. G. Nuzzo, L. Mahadevan, and J. A. Lewis, Nat. Mater. **15**, 413 (2016).
[27] T. H. Ware, M. E. McConney, J. J. Wie, V. P. Tondiglia, and T. J. White, Science **347**, 982 (2015).
[28] C. Mostajeran, M. Warner, T. H. Ware, and T. J. White, Proc. R. Soc. A **472**, 20160112 (2016).
[29] H. Aharoni, Y. Xia, X. Zhang, R. D. Kamien, and S. Yang, Proc. Natl. Acad. Sci. U.S.A. **115**, 7206 (2018).
[30] M. Warner and C. Mostajeran, Proc. R. Soc. A **474**, 20170566 (2018).
[31] B. A. Kowalski, C. Mostajeran, N. P. Godman, M. Warner, and T. J. White, Phys. Rev. E **97**, 012504 (2018).
[32] E. Siéfert and M. Warner, Proc. R. Soc. A **476**, 20200047 (2020).
[33] D. Duffy and J. S. Biggins, Soft Matter **16**, 10935 (2020).
[34] F. Feng, J. S. Biggins, and M. Warner, Phys. Rev. E **102**, 013003 (2020).
[35] E. Siéfert, E. Reyssat, J. Bico, and B. Roman, Nat. Mater. **18**, 24 (2019).
[36] A. Giudici and J. S. Biggins, J. Appl. Phys. **129**, 154701 (2021).
[37] I. Niv and E. Efrati, Soft Matter **14**, 424 (2018).
[38] See Supplemental Material at http://link.aps.org/supplemental/10.1103/PhysRevLett.127.128001 for additional information on the integration scheme and the elastic energy density.

[39] By definition, ϵ is a designable elastic feature so that either $\partial_\epsilon \lambda_1 \neq 0$ or $\partial_\epsilon \lambda_2 \neq 0$. Without loss of generality, we take $\partial_\epsilon \lambda_1 \neq 0$. Otherwise, $\partial_\epsilon \lambda_2 \neq 0$ and, by exchanging the director $\hat{\mathbf{n}}$ with $\hat{\mathbf{n}}_\perp$, we rename λ_2 as λ_1. Furthermore, it is sufficient that, only for one value of the actuation, $\Lambda = \Lambda_1$ and $\partial_\epsilon \lambda_1(\epsilon, \Lambda_1) \neq 0$.

[40] J. Hadamard, *Lectures on Cauchy's Problem in Linear Partial Differential Equations* (Yale University, New Haven, CT, 1923).

[41] L. C. Evans, *Partial Differential Equations*, 2nd ed. (American Mathematical Society, Providence, 2010), Vol. 19.

[42] Cauchy-Kovalevskaya theorem, Encyclopedia of Mathematics, https://encyclopediaofmath.org/wiki/Cauchy-Kovalevskaya_theorem.

[43] W. H. Press, S. A. Teukolsky, W. T. Vettering, and B. P. Flannery, Numerical Recipes: The Art of Scientific Computing, 3rd ed. (Cambridge University Press, USA, 2007).

[44] E. Goursat, *Cours D'Analyse Mathématique* (Gauthier-Villars, Paris, 1923), Vol. 3.

[45] H. Finkelmann, E. Nishikawa, G. G. Pereira, and M. Warner, Phys. Rev. Lett. **87**, 015501 (2001).

[46] E. M. Purcell, Am. J. Phys. **45**, 3 (1977).

[47] C. D. Modes, K. Bhattacharya, and M. Warner, Proc. R. Soc. A **467**, 1121 (2011).

[48] E. Efrati, E. Sharon, and R. Kupferman, J. Mech. Phys. Solids **57**, 762 (2009).

[49] I. Griniasty, Multi-surface inverse design: Calculating the designable properties of a uniaxial sheet (2021), https://doi.org/10.5281/zenodo.5146071.

[50] A. D. Auguste, J. W. Ward, J. O. Hardin, B. A. Kowalski, T. C. Guin, J. D. Berrigan, and T. J. White, Adv. Mater. **30**, 1802438 (2018).

[51] A. S. Kuenstler, Y. Chen, P. Bui, H. Kim, A. DeSimone, L. Jin, and R. C. Hayward, Adv. Mater. **32**, 2000609 (2020).

[52] Q. Liu, W. Wang, H. Sinhmar, A. Cortese, I. Griniasty, M. Reynolds, M. Taghavi *et al.*, *Electrically Programmable Micro-Scale Morphing Robots Based on Mechanical Metamaterials* (APS, 2021), https://meetings.aps.org/Meeting/MAR21/Session/Y14.1.

[53] M. Z. Miskin, K. J. Dorsey, B. Bircan, Y. Han, D. A. Muller, P. L. McEuen, and I. Cohen, Proc. Natl. Acad. Sci. U.S.A. **115**, 466 (2018).

[54] B. Bircan, M. Z. Miskin, R. J. Lang, M. C. Cao, K. J. Dorsey, M. G. Salim, W. Wang, D. A. Muller, P. L. McEuenA, and I. Cohen, Nano Lett. **20**, 4850 (2020).